Desalination and Water Treatment
www.deswater.com
doi: 10.1080/19443994.2014.991944

57 (2016) 4624–4632
February

Taylor & Francis
Taylor & Francis Group

Simultaneous biosorption of the two synthetic dyes, Direct Red 89 and Reactive Green 12 using nonliving macrophyte *L. gibba* L.

Samira Guendouz[a,b], Nabila Khellaf[a,b,*], Hayet Djelal[c,d], Moussa Ouchefoun[a,b]

[a]*Laboratory of Environmental Engineering, Faculty of Engineering, Badji Mokhtar University, P.O. Box 12, 23000 Annaba, Algeria, Tel./Fax: +213 38 87 65 60; emails: guendouzs@yahoo.fr (S. Guendouz), khellafdaas@yahoo.fr (N. Khellaf), ouchefoun-m@univ-annaba.com (M. Ouchefoun)*
[b]*Faculty of Engineering, Department of Process Engineering, Badji Mokhtar University, P.O. Box 12, 23000 Annaba, Algeria*
[c]*Ecole des Métiers de l'Environnement, Campus de Ker Lann, 35170 Bruz, France, email: hayetdjelal@ecole-eme.fr*
[d]*Université Européenne de Bretagne, 5 Boulevard Laennec, Rennes, France*

Received 21 April 2014; Accepted 19 November 2014

ABSTRACT

This study puts into light the capacity of *Lemna gibba* biomass (LGB) to be used as an effective biosorbent for the simultaneous removal of dyes from contaminated waters. The experiment was carried out at the laboratory scale and focuses on the single and binary biosorption of textile dyes. Direct Red 89 (DR-89) and Reactive Green 12 (RG-12)—two azo dyes—were treated with LGB which was selected as a biosorbent. The results showed that very acidic pH value (pH 1) was the optimal value for dye biosorption. When the aqueous system was charged with the two dyes (≥15 mg/L), the biosorption capacity of each individual dye decreased and the sorption capacity of LGB was reduced by 15%. The kinetic modeling results proved that the single biosorption of DR-89 and RG-12 was better accounted for by the pseudo-second-order ($R^2 > 0.96$). When the two organic pollutants were simultaneously present in the solution, the kinetic process well fitted the pseudo-second-order and pseudo-first-order models for removing, respectively, DR-89 and RG-12 from the mixture.

Keywords: Duckweed biomass; Kinetic modeling; Simultaneous biosorption; Pollutant mixture; Wastewater treatment

1. Introduction

In environmental studies dealing with pollution treatment processes, we often need a kinetic model to explain the mechanism of the physical, chemical, and/or biological phenomenon occurring during the treatment. It enables mathematical equations to be developed in order to represent and interpret experimental data, and also to evaluate the performance of the target process when applied in a large scale. The treatment process is characterized by the experimental kinetic data since they can track the progress of the process. Thus, the dynamic evolution curve usually representing mathematical equations produces information. The results of the simulation of these equations can interpret and analyze experimental data, and predict responses, thanks to the changes in the operational conditions and process optimization [1].

Several mathematical models were developed to kinetically assess the progression pattern of the process. The models were inferred thanks to a series

*Corresponding author.

of mass balance equations representing the concentration (or the relative rate) changes with respect to time. During sorption processes in a fluid-solid phase—also known as transformation operations—several patterns were applied in order to account for this stage that controls the kinetic process (external diffusion and intraparticle diffusion). It usually proceeds in three consecutive steps [1,2]: (i) The solute transport from the bulk of the solution to the surface of the particle, (ii) the solute transfer within the film surrounding the particle, and (iii) the diffusion inside the particle. The patterns commonly used are pseudo-first-order, pseudo-second-order, Elovich, and intraparticle diffusion patterns. These should be tested with a series of further experiments in order to be judged suitable. These kinetic patterns are mainly applied to single-solute biosorption in batch systems [3,4] and rarely to mixtures [5–7]. It is important to take the modeling of multi-compounds biosorption into account as a major step in the design of treatment systems.

Biosorption is a physicochemical process involving the retention of pollutant molecules on the surface of a biological device. It was tackled in many recent researches [8,9] and can be carried out through a number of independent processes including physical and chemical adsorption, ion exchange, complexation, chelation, and microprecipitation. It proves better than other wastewater treatment techniques because it is efficient, easily operated, simply designed, and cheap. It is already recognized as a potential excavenger for various types of pollutants [10–12] like dyes, for example, whose effects on humans, animals, and the various ecosystems were demonstrated and reviewed by several researchers [13,14].

The biosorption rate depends on several parameters: the state of the solid and the liquid phase, the physicochemical conditions (pH, temperature, agitation rate, and contact time), and the competitive compounds in the solution, since pollutants seldom exist on their own in wastewaters [7,15]. In particular, the combined effects on biosorption of two or more components depend on the combination of the pollutants as well as the level of pollutant concentration [16]. All these parameters influence the intensity of electrostatic effects occurring in the fluid–solid interface. The present study aims at assessing the kinetic bioremoval of two selected synthetic dyes (Direct Red 89 (DR-89) and Reactive Green 12 (RG-12)) in a single and binary system. The four kinetic patterns mentioned above were tested on the experimental data and used for (a) explaining the mechanism of dye disappearance from the contaminated medium and (b) studying the competitiveness of one dye biosorption in the presence of the other. The selected LGB as a biosorbent has some advantages because it can be easily found and provided by nature and it is easy to manipulate in laboratories. Furthermore, biomasses originated from various aquatic plants were successfully used as materials to remove pollutants (dyes, metal ions, and various types of pollutants) from wastewaters [17–19].

2. Materials and methods

2.1. Chemicals and biosorbent

The two dyes, DR-89 and RG-12, procured from the textile manufacture of Constantine (Algeria) were used without further purification. Their chemical structures are shown on Fig. 1. Their physicochemical data were detailed in our previous study [20].

The other chemicals (HCl and NaOH used for adjusting solution pH) were purchased from Merck. All the solutions were prepared using distilled water (pH 6.5). The biosorbent material, used without any pretreatment, consisted of *Lemna gibba* biomas (LGB). The protocol of prepared biosorbent was well previously described by Guendouz et al. [20].

2.2. Kinetic biosorption experiments

Biosorption assays (in duplicate) were conducted under static conditions in 1 L capacity thermostated glass reactors. Treatments and controls were continuously stirred at 200 rpm and 20°C for 2 h in the presence of 2 g of LGB. Initial pH of solution adjusted with 1 M HCl or 1 M NaOH was measured with a pH-meter model HANNA 211. At defined time intervals ranging from 1 to 5 min, a 2 mL aliquot of each sample was taken from the reactors and diluted with distilled water; the sample was centrifuged at 3,000 rpm during 10 min before analyzing the supernatant. The dye concentration (in single and binary system) was evaluated by measuring the absorbance using a UV–vis spectrophotometer (WPA lightwave II). The details of measurements were explained in Section 3.1. The effect of pH (1, 7, and 13) on the kinetic biosorption of monosolute solution dye was investigated with 5–15 mg L^{-1} as initial dye concentrations. pH value of 1 was chosen to investigate the kinetic biosorption of bisolute solution dye using nine different binary solutions (Table 1). All the assays were followed by calculating the biosorption capacity at equilibrium, Q_e (mg/g) and at time t, Q_t (mg/g).

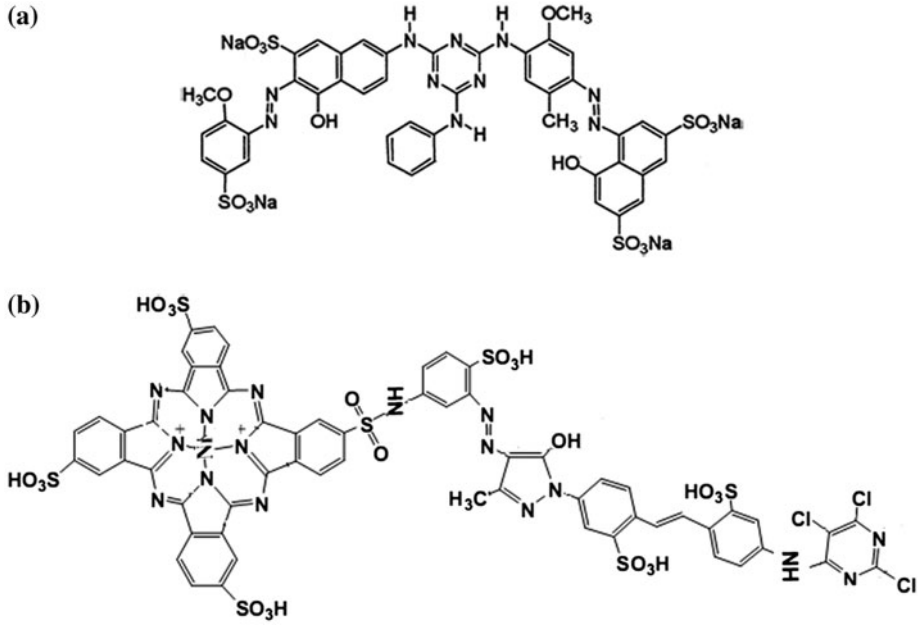

Fig. 1. Chemical structure of (a) DR-89 and (b) RG-12 dyes.

Table 1
Composition of the binary systems of DR-89 and RG-12

Binary system	Composition
DR5 + RG5	5 mg/L DR-89 + 5 mg/L RG-12
DR5 + RG10	5 mg/L DR-89 + 10 mg/L RG-12
DR5 + RG15	5 mg/L DR-89 + 15 mg/L RG-12
DR10 + RG5	10 mg/L DR-89 + 5 mg/L RG-12
DR10 + RG10	10 mg/L DR-89 + 10 mg/L RG-12
DR10 + RG15	10 mg/L DR-89 + 15 mg/L RG-12
DR15 + RG5	15 mg/L DR-89 + 5 mg/L RG-12
DR15 + RG10	15 mg/L DR-89 + 10 mg/L RG-12
DR15 + RG15	15 mg/L DR-89 + 15 mg/L RG-12

2.3. Kinetic modeling

The main objective of this study was the kinetic modeling of DR-89 and RG-12 biosorption both in single and binary system. The study was carried out on four mathematical equations: the pseudo-first-order, pseudo-second-order, Elovich and intraparticle diffusion models. These models are used as empirical relations between the variation of sorption capacity of the sorbate (dye) and the time of exposure. The four models and their linearized forms (obtained by separating variables and integrating) are represented by the following relationships:

Pseudo-first-order model:

$$\frac{dQ_t}{dt} = k_1(Q_e - Q_t) \Rightarrow \ln(Q_e - Q_t) = \ln Q_e - k_1 t \quad (1)$$

Pseudo-second-order model:

$$\frac{dQ_t}{dt} = k_2(Q_e - Q_t)^2 \Rightarrow \frac{t}{Q_t} = \frac{1}{k_2 Q_e^2} + \frac{1}{Q_e} t \quad (2)$$

Elovich model:

$$\frac{dQ_t}{dt} = \alpha \exp(-\beta Q_t) \Rightarrow Q_t = \frac{1}{\beta}\ln(\alpha\beta) + \ln t \quad (3)$$

Intraparticle diffusion model:

$$Q_t = K_{id} t^{1/2} + C \quad (4)$$

k_1 (min^{-1}) and k_2 (g/mg min) are the rate constants of the pseudo-first-order and pseudo-second-order models, respectively,

α (mg/g min) and β (g/mg) are, respectively, the initial sorption rate and desorption constants in the Elovich model, and

K_{id} (mg/g $min^{1/2}$) is the intraparticle diffusion rate constant.

The different constants describing the four kinetic models can be evaluated by slops and intercepts obtained from the plot of the first term (in the linearized forms) against t (or $t^{1/2}$ in the case of Eq. (4)). The coefficient of determination (R^2) and some calculated parameters (compared to the experimental

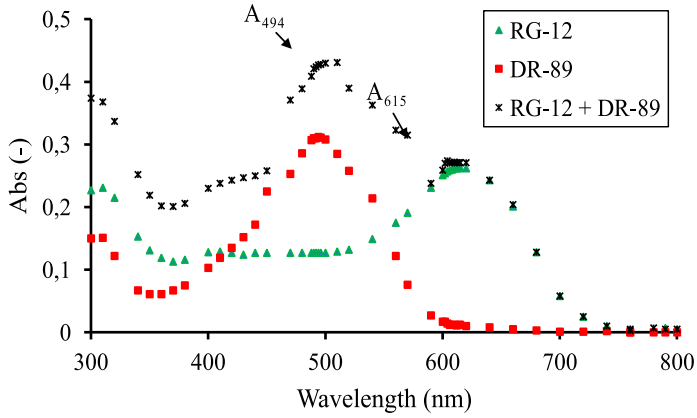

Fig. 2. Absorption spectra in UV–vis of DR-89 and RG-12 dyes in single and binary system ($C_{DR\text{-}89}$ = 15 mg/L, $C_{RG\text{-}12}$ = 15 mg/L).

parameters) were chosen as the criterion for determining the more suitable model that can describe the experimental data of the present study [21,22].

3. Results and discussion

3.1. Simultaneous analysis of DR-89 and RG-12 in binary system

Dye concentration in single system was evaluated by measuring the absorbance at the maximal wavelength of each dye. Calibration curves were established prior to the analysis. When the two dyes were simultaneously present in solution (binary system), the law of additivity of absorbances (Lambert and Beer's law) was applied. The absorption spectra of the two dyes were separately recorded between the wavelength ranges of 300–800 nm. As can be seen on Fig. 2, the maximal wavelength of DR-89 and RG-12 were 494 and 615 nm, respectively, and the two spectra overlapped for a wavelength lower than 500 nm. Thus, the DR-89 concentration can be determined at 615 nm in the presence of RG-12 where its absorbance is zero. On the other hand, the two spectra overlapped at 495 nm where the binary solution absorbance is equal to the sum of absorbances of the two dyes. The unknown concentrations of the two dyes simultaneously present in solution are determined by solving the following system (Fig. 2):

$$\begin{cases} A_{615} = \varepsilon_{RG}^{615} C_{RG} L \\ A_{494} = \varepsilon_{DR}^{494} C_{DR} L + \varepsilon_{RG}^{494} C_{RG} L \end{cases} \quad (5)$$

The solutions of the above-mentioned mathematical system representing the concentration of DR-89 and RG-12, respectively,

$$C_{RG} = \frac{A_{615}}{\varepsilon_{RG}^{615} L} \quad (6)$$

$$C_{DR} = \frac{A_{494} - \varepsilon_{RG}^{494} C_{RG} L}{\varepsilon_{DR}^{494} L} \quad (7)$$

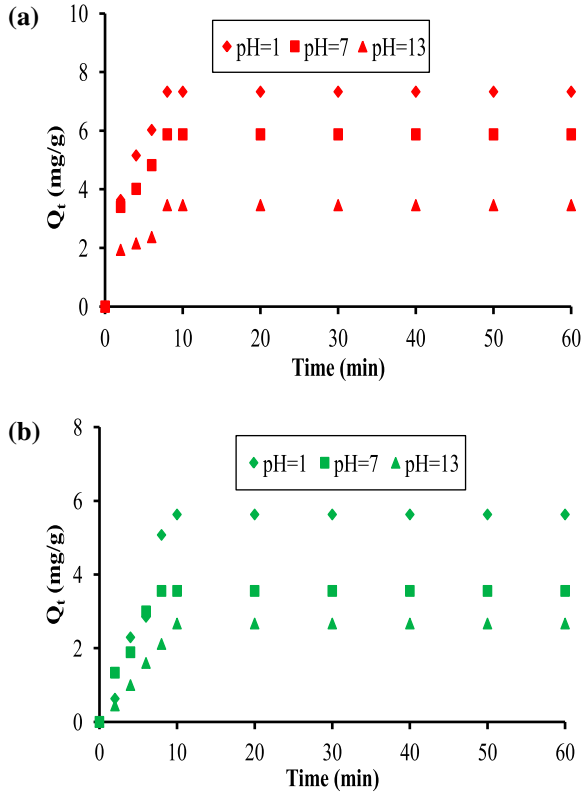

Fig. 3. Effect of pH on LGB biosorption capacity of (a) DR-89 and (b) RG-12 dyes in monosolute system ($C_{DR\text{-}89}$ = 15 mg/L, $C_{RG\text{-}12}$ = 15 mg/L).

A_{615} and A_{494} are the binary system absorbances at the wavelength of 615 and 494 nm, respectively,

ε_{RG}^{615}, ε_{RG}^{494} and ε_{DR}^{494} are the molar extinction coefficients of the two dyes; their values are deduced from the calibration curves established at 615 and 494 nm for RG-12 and at 494 nm for DR-89, respectively,

L is the length of the glass cell ($L = 1$ cm).

3.2. Kinetic of dye abatement for different initial pH

Preliminary essays demonstrated that the variation of solution initial pH had negligible effect on the maximal absorption wavelength (λ_{max}) of DR-89 and RG-12 (Data not shown). Three initial pH values (1, 7, and 13) were selected for assessing the effect of solution pH on dye biosorption in monosolute system. These experiments were necessary to know the optimal value of pH at which the bisolute essays might be conducted. Fig. 3 exhibiting the abatement of DR-89 (Fig. 3(a)) and RG-12 (Fig. 3(b)) in single system during the exposure time showed that maximum biosorption (mg/g) were obtained at pH 1. At neutral and basic pH, biosorption capacity of LGB decreased and attained, respectively, 5.87 and 3.46 mg/g for DR-89.

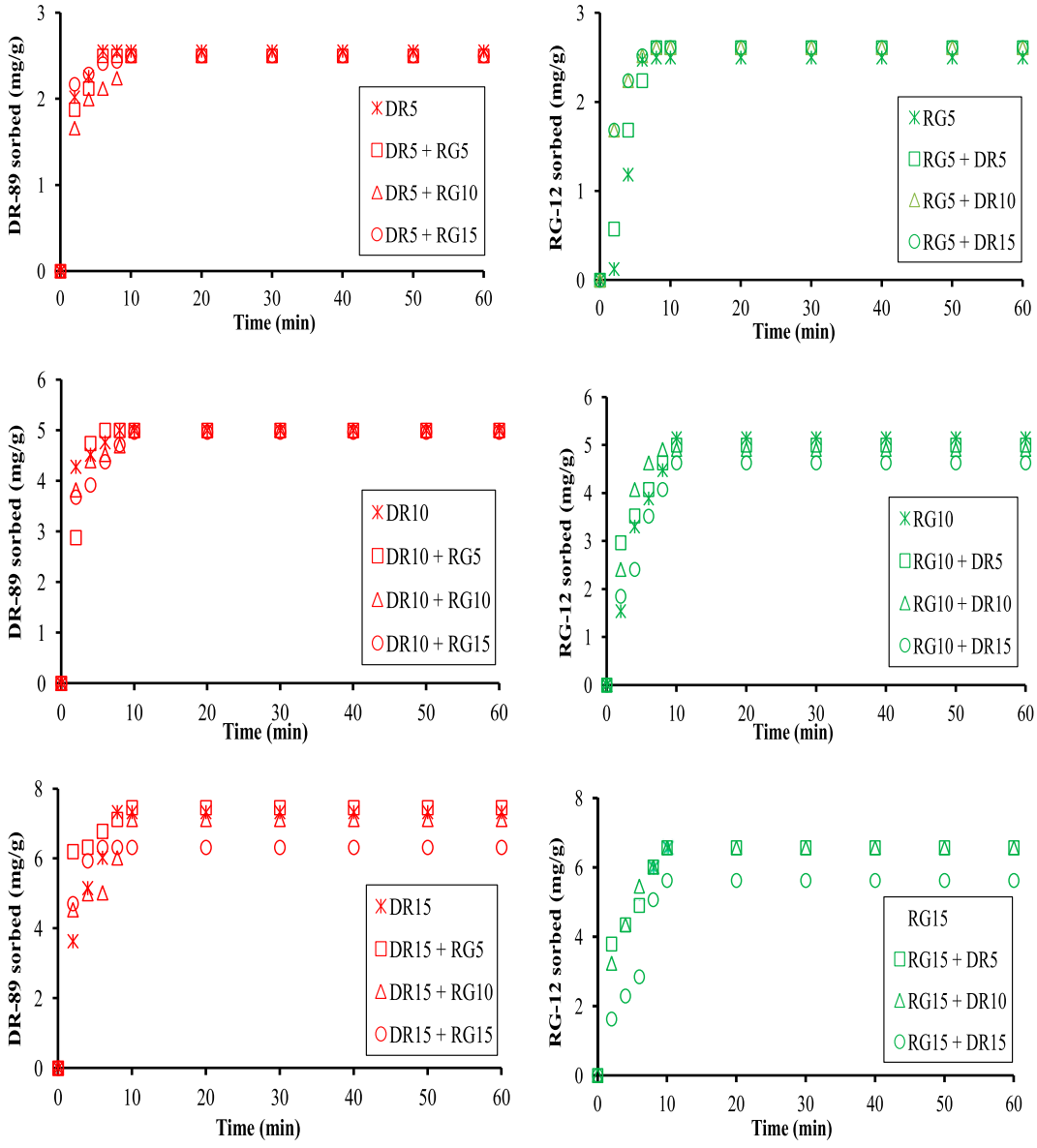

Fig. 4. Simultaneous biosorption of DR-89 (in red) and RG-12 (in green) by dried LGB. The composition of the different binary systems is given in Table 2.

Similar trend was observed for RG-12 with a maximum biosorption of 7.75 mg/g (at pH 1). These results showed that the biosorption capacity of LGB decreased with increasing pH values. Similar results were found in other studies where the authors demonstrated that maximum biosorption of dyes was reached at low pH values [23,24]. This fact may be due to a competition between OH^- ions (under basic conditions) and the anionic dyes (with their sulfonate groups, SO_3^-) or an increase in the electrostatic repulsion of the anionic dye species by the negatively charged biomass surface under basic conditions [22,25,26]. According to other thesis, the greater removal of anionic dyes under acidic media might be referred to availability of more cationic sites on the biosorbent surface [23].

3.3. Simultaneous biosorption of DR-89 and RG-12 in binary system

Competitive biosorption of one dye in the presence of other dye was studied and compared with the monosolute biosorption. Fig. 4 representing the binary system biosorption of DR-89 and RG-12 showed as a first result that the duckweed biomass showed ability in sorbing dyes simultaneously. Additionally, the same figure showed that sorption capacity of one dye was not affected by the presence of other dye when the concentration of at least one dye was lower than 15 mg/L. In this case, all dye molecules present in the solution could interact with the binding sites. When the aqueous system was charged with 15 mg/L DR-89 and 15 mg/L RG-12, biosorption capacity of individual dye decreased from 7.50 to 6.12 mg/g and from 6.80 to 5.72 mg/g for DR-89 and RG-12, respectively. Hence, the dye effect on the removal process became pronounced as the other dye concentration in solution exceeded 10 mg/L. The sorption capacity of LGB was reduced by approximately 15% in the presence of the two dyes. Our results are different from those of Dawood and Sen [26] since the authors confirmed that the biosorption capacity of a fungal biomass in binary system (100 mg/L Acid Blue 25 and 100 mg/L Acid Blue 337) was significantly lower than the adsorption capacity in single system at pH 2–5. Similarly, in a study of the competitive biosorption of Acid Red 274 and Acid Red 337 using green algae, the authors observed that the uptake amounts of the first component decreased with increasing concentration of the second component from binary solution; the combined biosorption was found as antagonistic behavior resulting in a lower biosorption yield [16]. The difference with our results is probably due to the fact that the pollutant charge was lower in our study. Testing high concentrations of dyes (mainly RG-12) was not feasible

Table 2
Constants deduced from the kinetic analysis of biosorption of DR-89 and RG-12 in mono-solute system

Kinetic model	DR-89			RG-12		
	5 mg/L	10 mg/L	15 mg/L	5 mg/L	10 mg/L	15 mg/L
Pseudo-first-order						
k_1 (min^{-1})	0.276	0.263	0.230	0.268	0.241	0.195
$Q_{e\ cal}$ (mg/g)	2.489	3.815	5.228	2.428	5.243	5.966
$Q_{e\ exp}$ (mg/g)	2.504	4.135	5.875	2.390	4.330	3.560
R^2	0.999	0.935	0.961	0.984	0.979	0.935
Pseudo-second-order						
k_2 (g/mg min)	0.391	0.396	0.422	1.239	1.136	2.602
$Q_{e\ cal}$ (mg/g)	2.577	4.132	5.917	2.558	4.310	3.676
$Q_{e\ exp}$ (mg/g)	2.455	4.135	5.875	2.390	4.330	3.560
R^2	*0.983*	*0.999*	*0.961*	*0.988*	*0.971*	*0.993*
Elovich						
α (mg/g min)	0.000	1.203	2.010	1.508	1.002	0.000
β (g/mg)	1.152	1.203	1.693	0.521	1.344	1.670
R^2	0.924	0.784	0.903	0.903	0.948	0.947
Intraparticle diffusion						
k_{id} (mg/g $min^{1/2}$)	0.814	1.345	2.000	1.025	1.332	1.144
C (mg/g)	0.000	0.056	0.144	0.132	0.052	0.000
R^2	0.933	0.964	0.986	0.953	0.995	0.914

Note: $Q_{e\ cal}$ and $Q_{e\ exp}$ are respectively the calculated and the experimental capacity biosorption of LGB at equilibrium. Italic values correspond to the higher coefficients of determination.

in this work because the efficacy of using LGB for the bioremoval of the reactive dye was limited to concentrations ≤15 mg/L (see our previous study).

On the other hand, as shown in Fig. 4, LGB showed quite different efficiency toward the two dyes (DR-89 > RG-12) that has to be related to their different chemical structures. The green dye (RG-12) has higher molecular weight which made it less attractable by biosorption [15].

3.4. Modeling

To understand the mechanism of the present phenomenon, the experimental data were applied according to the four kinetic equations indicated above. Biosorption kinetic models for the two dyes were obtained at pH 1 in single and binary systems. The applicability of a model is subject to obtain a straight line with a higher coefficient of determination and the concordance of the predicted and the experimental data. The calculated and experimental kinetic parameters in single system are summarized in Table 2. The low values of R^2 and the difference between the experimental and the calculated sorption capacity (Q_e) indicate that the pseudo-first-order and Elovich models were not suitable for describing the removal of both dyes using LGB. Pseudo-second-order ($R^2 > 96\%$) was able to describe the experimental data

Table 3
Constants deduced from the kinetic analysis of biosorption of DR-89 (in bold) and RG-12 (in normal) in binary systems

	Kinetic constants								
Kinetic model	DR5 + RG5	DR5 + RG10	DR5 + RG15	DR10 + RG5	DR10 + RG10	DR10 + RG15	DR15 + RG5	DR15 + RG10	DR15 + RG15
Pseudo-first-order									
k_1 (min^{-1})	**0.480**	**0.482**	**0.717**	**0.754**	**0.551**	**0.409**	**0.699**	**0.340**	**0.197**
	0.332	0.299	0.272	0.550	0.499	0.302	0.550	0.258	0.289
$Q_{e\ cal}$ (mg/g)	**2.223**	**1.876**	**1.889**	**6.475**	**3.522**	**3.651**	**6.385**	**4.660**	**5.414**
	3.146	4.604	6.147	2.779	6.123	6.613	2.779	4.978	5.352
$Q_{e\ exp}$ (mg/g)	**2.595**	**2.610**	**2.435**	**5.350**	**5.000**	**4.965**	**6.320**	**7.456**	**6.120**
	3.161	4.500	6.020	2.610	5.962	6.575	2.610	4.630	5.725
R^2	**0.928**	**0.977**	**0.959**	**0.951**	**0.949**	**0.923**	**0.999**	**0.878**	**0.851**
	0.948	*0.970*	0.928	*0.991*	*0.984*	*0.993*	*0.991*	*0.971*	*0.974*
Pseudo-second-order									
k_2 (g/mg min)	**0.420**	**0.376**	**0.152**	**0.311**	**0.205**	**0.149**	**0.107**	**0.102**	**0.058**
	0.172	0.162	0.119	0.267	0.125	0.110	0.311	0.136	0.091
$Q_{e\ cal}$ (mg/g)	**2.525**	**2.660**	**2.558**	**6.757**	**5.051**	**5.263**	**6.897**	**7.937**	**6.197**
	1.495	2.331	2.604	1.828	2.222	2.320	1.828	1.026	1.597
$Q_{e\ exp}$ (mg/g)	**2.595**	**2.610**	**2.435**	**6.350**	**5.000**	**4.965**	**6.320**	**7.456**	**6.120**
	3.161	4.500	6.020	2.610	5.962	6.575	2.610	4.630	5.725
R^2	***0.993***	***0.999***	***0.999***	***0.973***	***0.999***	***0.991***	***0.997***	***0.995***	***0.995***
	0.995	0.983	0.949	0.998	0.981	0.992	0.998	0.911	0.966
Elovich									
α (mg/g min)	**1.555**	**2.027**	**1.388**	**2.382**	**3.442**	**3.074**	**4.241**	**5.486**	**3.219**
	0.235	1.942	2.292	0.377	1.514	1.669	0.377	0.380	0.723
β (g/mg)	**0.545**	**0.200**	**0.414**	**1.577**	**0.617**	**0.738**	**1.017**	**0.781**	**1.404**
	1.300	1.269	1.719	1.204	1.630	2.096	1.204	1.766	2.467
R^2	**0.926**	**0.980**	**0.991**	**0.859**	**0.967**	**0.919**	**0.859**	**0.883**	**0.740**
	0.988	0.965	0.897	0.896	0.943	0.989	0.896	0.949	0.970
Intraparticle diffusion									
k_{id} (mg/g $min^{1/2}$)	**1.067**	**0.804**	**0.871**	**2.020**	**1.686**	**1.653**	**2.034**	**2.250**	**2.057**
	0.595	1.555	2.011	0.956	1.680	2.099	0.956	1.467	2.104
C (mg/g)	**0.130**	**0.205**	**0.345**	**0.272**	**0.557**	**0.464**	**0.915**	**1.201**	**0.550**
	0.000	0.292	0.300	0.148	0.183	0.127	0.148	0.000	0.000
R^2	**0.962**	**0.930**	**0.849**	**0.973**	**0.889**	**0.917**	**0.873**	**0.845**	**0.932**
	0.920	0.977	0.977	0.698	0.964	0.996	0.698	0.986	0.994

Note: $Q_{e\ cal}$ and $Q_{e\ exp}$ are respectively the calculated and the experimental capacity biosorption of LGB at equilibrium. Italic values correspond to the higher coefficients of determination.

related to DR-89 biosorption; the experimental and theoretical values of dye sorption capacity (Q_e) were in accordance with each other. The same kinetic model represented well the biosorption of RG-12 with satisfactory coefficients of determination ($R^2 > 97\%$). Additionally, these results related to the importance of diffusion into LGB, showed that the intraparticle diffusion was the rate-limiting step in dye biosorption because the function $Q_t = f(t^{1/2})$ is linear; however, this function doesn't pass though the origin ($C \neq 0$), then, the intraparticle diffusion is not the only rate-limiting step that control the rate of the adsorption process.

In the case of the binary systems, the parameters obtained from the linear curve fit of the four models with experimental data are listed in Table 3. Regarding the different coefficients of determination and the calculated Q_e, it can be concluded that pseudo-second-order and pseudo-first-order models successfully predicted the biosorption kinetic of DR-89 and RG-12, respectively. The experimental and theoretical values of dye sorption capacity (Q_e) were in accordance with each other when the data were modeled with these kinetic equations. Also, the rate-limiting step in the binary dye sorption was the intraparticle diffusion without being the only limiting step in the control of the global rate of the process.

On the other hand, as predicted by the pseudo-first-order and pseudo-second-order models, it was observed that biosorption kinetic of RG-12 was slower than that of DR-89 when present at low concentration in the aqueous medium. This fact might be due to the molecular weight of the green dye which is higher than that of the red dye. The value of the rate constants (Table 3) was higher in the case of DR-89 biosorption for most concentrations tested in this work. The biosorbent showed a preference for sorbing DR-89 over RG-12 indicating that LGB gave priority to DR-89 at initial stage.

4. Conclusion

This study deals with the single and combined biosorption of two synthetic dyes—Direct Red 89 and Reactive Green 12—using the *L. gibba* dried biomass. During the experiments, we observed that the duckweed biomass could sorb dyes simultaneously, and the efficiency of the dye on the removal process became lower as the other dye concentration in solution exceeded 10 mg/L. The kinetic modeling revealed that the pseudo-second-order pattern successfully described the DR-89 and RG-12 removal in a monosolute solution. When the two compounds were simultaneously present in the solution, the kinetic way for the bioremoval of RG-12 changed to the pseudo-first-order pattern. Finally, with a solution containing both DR-89 and RG-12, LGB gave priority to DR-89 at the initial stage of the biosorption.

Acknowledgments

The authors thank the Ministry of Higher Education and Scientific Research, Algeria for the financial support through the CNEPRU project.

References

[1] P. Marin, C.E. Borba, A.N. Módenes, F.R. Espinoza-Quiñones, S.P. Dias de Oliveira, A.D. Kroumov, Determination of the mass transfer limiting step of dye adsorption onto commercial adsorbent by using mathematical models, Environ. Technol. 35(17–20) (2014) 2356–2364.

[2] S. Attouti, B. Benaouda, N. Benderdouche, L. Duclaux, Application of *Ulva lactuca* and *Systoceira stricta* algae-based activated carbons to hazardous cationic dyes removal from industrial effluents, Water Res. 47 (2013) 3375–3388.

[3] C. Shuang, P. Li, A. Li, Q. Zhou, M. Zhang, Y. Zhou, Quaternized magnetic microspheres for the efficient removal of reactive dyes, Water Res. 46 (2012) 4417–4426.

[4] V.J.P. Vilar, M.S. Cidalia, R.A.R. Boaventura B, Kinetics modelling of biosorption by algal biomass from binary metal solutions using batch contactors, Biochem. Eng. J. 38 (2008) 319–325.

[5] N.M. Mahmoodi, R. Salehi, M. Arami, Binary system dye removal from colored textile wastewater using activated carbon: Kinetic and isotherm studies, Desalination 272 (2011) 187–195.

[6] N.M. Mahmoodi, J. Abdi, F. Najafi, Gemini polymeric nanoarchitecture as a novel adsorbent: Synthesis and dye removal from multicomponent system, J. Colloid Interface Sci. 400 (2013) 88–96.

[7] M. Ghaedi, S. Hajati, B. Barazesh, F. Karimi, G. Ghezelbash, *Saccharomyces cerevisiae* for the biosorption of basic dyes from binary component systems and the high order derivative spectrophotometric method for simultaneous analysis of Brilliant green and Methylene blue, J. Ind. Eng. Chem. 19(1) (3013) 227–233.

[8] A. Mittal, V. Thakur, J. Mittal, H. Vardhan, Process development for the removal of hazardous anionic azo dye Congo red from wastewater by using hen feather as potential adsorbent, Desalin. Water Treat. 52 (2014) 227–237.

[9] H. Daraei, A. Mittal, M. Noorisepehr, J. Mittal, Separation of chromium from water samples using eggshell powder as a low-cost sorbent: Kinetic and thermodynamic studies, Desalin. Water Treat. 2014 (in press), doi: 10.1080/19443994.2013.837011.

[10] A. Mittal, J. Mittal, L. Kurup, A.K. Singh, Process development for the removal and recovery of hazardous dye erythrosine from wastewater by waste materials-bottom ash and de-oiled soya as adsorbents, J. Hazard. Mater. B 138 (2006) 95–105.

[11] H. Daraei, A. Mittal, J. Mittal, H. Kamali, Optimization of Cr(VI) removal onto biosorbent eggshell membrane: Experimental & theoretical approaches, Desalin. Water Treat. 52 (2014) 1307–4315.
[12] J. Mittal, D. Jhare, H. Vardhan, A. Mittal, Utilization of bottom ash as a low-cost sorbent for the removal and recovery of a toxic halogen containing dye eosin yellow, Desalin. Water Treat. 52 (2014) 4508–4519.
[13] V.K. Gupta, R. Jain, A. Mittal, M. Mathur, S. Shalini, Photochemical degradation of the hazardous dye Safranin-T using TiO_2 catalyst, J. Colloid Interface Sci. 309 (2007) 464–469.
[14] J. Mittal, V. Thakur, A. Mittal, Batch removal of hazardous azo dye Bismark Brown R using waste material hen feather, Ecol. Eng. 60 (2013) 249–253.
[15] E. Daneshvar, M. Kousha, M.S. Sohrabi, A. Khataee, A. Converti, Biosorption of three acid dyes by the brown macroalga *Stoechospermum marginatum*: Isotherm, kinetic and thermodynamic studies, J. Chem. Eng. 195–196 (2012) 297–306.
[16] A. Ozer, M. Turabik, Competitive biosorption of acid dyes from binary solutions onto *Enteromorpha prolifera*: Application of the first order derivative spectrophotometric analysis method, Sep. Sci. Technol. 45 (2010) 380–393.
[17] M. Kousha, E. Daneshvar, A.R. Esmaeili, H. Zilouei, K. Karimi, Biosorption of toxic acidic dye-Acid Blue 25, by aquatic plants, Desalin. Water Treat. 52(34–36) (2014) 6756–6769.
[18] P. Miretzky, A. Saralegui, A.F. Cirelli, Simultaneous heavy metal removal mechanism by dead macrophytes, Chemosphere 62 (2006) 247–254.
[19] L. Chen, Y. Fang, Jin, Q. Chen, Y. Zhao, Y. Xiao, H. Zhao, Biosorption of Cd^{2+} by untreated dried powder of duckweed *Lemna aequinoctialis*, Desalin. Water Treat. 2014 (in press), doi: 10.1080/19443994.2013.839399.
[20] S. Guendouz, N. Khellaf, M. Zerdaoui, M. Ouchefoun, Biosorption of synthetic dyes (Direct Red 89 and Reactive Green 12) as an ecological refining step in textile effluent treatment, Environ. Sci. Pollut. Res. 20 (2013) 3822–3829.
[21] F.-C. Wu, R.-L. Tseng, R.-S. Juang, Characteristics of Elovich equation used for the analysis of adsorption kinetics in dye-chitosan systems, Chem. Eng. J. 150 (2009) 366–373.
[22] Z. Yaneva, N. Georgieva, Study on the physical chemistry, equilibrium, and kinetic mechanism of azure a biosorption by *Zea mays* biomass, J. Dispersion Sci. Technol. 35(2) (2014) 193–204.
[23] M. Asgher, H.N. Bhatti, Mechanistic and kinetic evaluation of biosorption of reactive azo dyes by free, immobilized and chemically treated *Citrus sinensis* waste biomass, Ecol. Eng. 36 (2010) 1660–1665.
[24] S.W. Won, M.H. Han, Y.-S. Yun, Different binding mechanisms in biosorption of reactive dyes according to their reactivity, Water Res. 42 (2008) 4847–4855.
[25] Y. Yang, D. Jin, G. Wang, S. Wang, X. Jia, Y. Yuhua, Zhao. competitive biosorption of Acid Blue 25 and Acid Red 337 onto unmodified and CDAB-modified biomass of *Aspergillus oryzae*, Bioresour. Technol. 102 (2011) 7429–7436.
[26] S. Dawood, T.K. Sen, Removal of anionic dye congo red from aqueous solution by raw pine and acid-treated pine cone powder as adsorbent: Equilibrium, thermodynamic, kinetics, mechanism and process design, Water Res. 46 (2012) 1933–1946.